

4-1-2002

Mathematical Modeling and Computer Simulation of the Rotating Impeller Particle Flotation Process: Part I. Fluid Flow

Mohammed D. Maniruzzaman

Makhlouf M. Makhlouf

Worcester Polytechnic Institute, mmm@wpi.edu

Follow this and additional works at: <https://digitalcommons.wpi.edu/mechanicalengineering-pubs>



Part of the [Mechanical Engineering Commons](#)

Suggested Citation

Maniruzzaman, Mohammed D. , Makhlouf, Makhlouf M. (2002). Mathematical Modeling and Computer Simulation of the Rotating Impeller Particle Flotation Process: Part I. Fluid Flow. *Metallurgical and Materials Transactions B-Process Metallurgy and Materials Processing Science*, 33(2), 297-303.

Retrieved from: <https://digitalcommons.wpi.edu/mechanicalengineering-pubs/29>

This Article is brought to you for free and open access by the Department of Mechanical Engineering at Digital WPI. It has been accepted for inclusion in Mechanical Engineering Faculty Publications by an authorized administrator of Digital WPI. For more information, please contact digitalwpi@wpi.edu.

Mathematical Modeling and Computer Simulation of the Rotating Impeller Particle Flotation Process: Part I. Fluid Flow

M. MANIRUZZAMAN and M. MAKHLOUF

Removal of unwanted particles from molten metal by flotation is one of the most useful melt cleansing techniques used by the foundry industry. An effective way of flotation of particles in a melt relies on purging a gas into the molten metal through holes in a rotating impeller. Impeller rotation creates turbulence inside the melt, which helps agglomerate the impurity particles and, thereby, enhances their removal from the melt. In addition, turbulence increases the probability of particles attaching to the rising gas bubbles and, therefore, enhances the chance of their removal from the molten metal. A mathematical model has been developed to simulate the turbulent multiphase flow field inside the flotation treatment furnace. Simulations based on the model were used to demonstrate the effect of the various process parameters on the performance of a batch-type rotating impeller particle flotation process.

I. INTRODUCTION

THE quality of cast products largely depends on effective treatment of the molten metal prior to casting in order to remove unwanted second phases. These *unwanted phases* include all exogenous solid particles and liquid phases that may be present above the liquidus temperature of the alloy, as well as all gaseous phases dissolved in the melt. When present in a cast product, second phases can cause a variety of property changes including increase in the modulus of elasticity^[1,2] reduction in the fatigue strength^[1,3-5] and ductility, increase in corrosion rate,^[1] and reduction in electrical and thermal conductivity.^[1,6] Solid inclusions that exist in aluminum foundry products can be classified into several general categories. These include oxides, carbides, intermetallic compounds, and many other exogenous refractory particles. In general, most of these solid inclusions exhibit complex structures and are very hard and brittle. The critical size of solid inclusions that may be tolerated in a casting depends on the end application. In most applications, inclusions with particle sizes greater than 10 to 20 μm have a drastic effect on the quality of the part. Flotation of these particles to the surface of the melt in a rotary degasser is an effective method of removing them from molten alloys. In this process, a reactive or inert gas, or a combination of both types of gases, is purged through a rotating impeller into the liquid metal. Figure 1 shows a typical rotating impeller flotation treatment process. While the gas, in the form of discrete bubbles, rises to the surface, it encounters the inclusions and carries them to the top slag. The efficiency of inclusion removal in a rotary degasser depends on the interaction between the bubbles and the metal. This interaction largely depends on the flow field inside the melt created by the flow of the bubble as well as by the impeller rotation. Inclusion removal also depends on the agglomeration of the

particles caused by turbulence in the flow field. The velocity and turbulence fields, largely, govern the transport of inclusions to the bubble surface.

Historically, the optimization of melt-treatment processes relied largely on operator experience, but better understanding of the process may be achieved through mathematical modeling and computer simulations. In addition, simulations may be used to optimize existing processes, design new processes, and determine causes and/or corrective actions for specific problems. However, the rotating impeller flotation treatment process is quite difficult to model since it encompasses a flow system that consists of multiple, separate, yet interacting, phases including a liquid phase (the molten alloy), a gaseous phase (the purged gas), and one or more solid phases (the inclusion particles). The difficulty of modeling such a system stems from the inability of current hardware to handle models that provide a detailed description of the flow field inside the reactor including the turbulence created by the impeller rotation and gas flow, the interaction between the liquid and gas phases, and the dynamics of the colliding particles. In order to simplify the analysis and make it amenable to solution, previous simulations of the process focused on the flow field induced by the injected gas bubbles.^[7,8,9] For example, Johansen *et al.*^[10] and Hop *et al.*^[11] in the simulation of a hydro gas-purging unit, modeled the flow field induced by the impeller by using single-phase transport equations. They assumed the purged gas, in the form of bubbles, was introduced into the computational domain as a dispersed phase, and its trajectory was then tracked using a Lagrangian approach. The inclusion removal efficiency was computed based on the bubble trajectories along with the theory of particle deposition onto bubbles.^[10,11] To further simplify the model, Johansen *et al.*^[10] and Hop *et al.*^[11] did not model the reactor's free surface and, consequently, excluded its effect on the flow field from the analysis.

We propose a different approach to modeling and simulating the rotary degasser. The complex flow system that consists of multiple interacting phases is modeled as two separate but interdependent subsystems. The first subsystem,

M. MANIRUZZAMAN, Postdoctoral Fellow, and M. MAKHLOUF, Associate Professor, are with the Materials Science and Engineering Department, Worcester Polytechnic Institute, Worcester, MA 01609.

Manuscript submitted May 11, 2000.

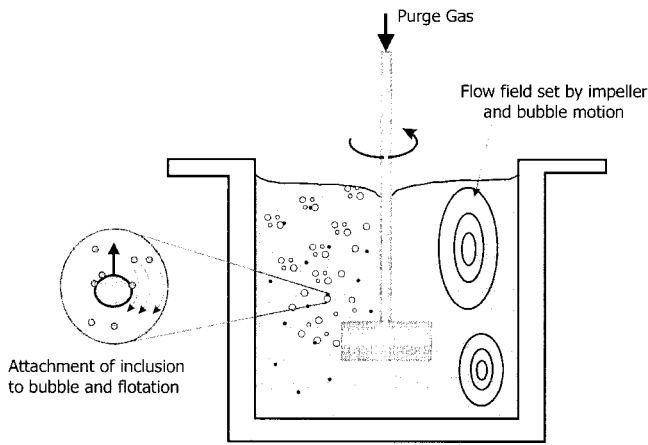


Fig. 1—Schematic diagram describing the various steps in the flotation treatment process.

which is the subject of this article, is the turbulent flow field arising from the impeller rotation and bubble flow. Standard fluid flow and turbulence equations are used in modeling this subsystem, and a special computational fluid dynamics (CFD) routine that uses an Eulerian multiphase approach and tracks the interface between the gas phase and the liquid phase is employed in the computer simulation. The second subsystem deals with particle collisions and particle to bubble attachment. A model of this subsystem, which is presented elsewhere,^[12] accepts input from the flow field simulation in the form of turbulence dissipation energy and bubble distribution and uses a special particle population balance to track the change in particle population with duration of the treatment process. By modeling the two subsystems separately, it is possible to include more complexity into the models without prohibitively taxing computer time. For example, unlike previous models, the current fluid flow model allows possible movement of the melt's free surface and, thus, can reflect any possible *vortexing* at the melt's surface. In this article, we present the fluid flow model and use it to simulate the performance of a batch-process rotary degasser.

II. THE MATHEMATICAL MODEL

The Euler-Euler method^[13,14] is used to formulate the mathematical model, and the volume of fluid (VOF) technique^[15] is used to solve the model equations. In the Euler-Euler method, the different phases are treated mathematically as interpenetrating continua where volume fractions of all phases are assumed continuous in space and time, and their sum is equal to one. By using the VOF technique, only one set of transport equations is needed, and the interface between the phases is defined by transport equations in which diffusion across the interfaces is not allowed. The use of the VOF technique allows modeling the free boundaries between phases. Free boundaries are considered to be free surfaces of the molten metal or interfaces between two fluids, such as the molten metal and the purging gas in the case of the flotation treatment process. The reason for the *free* designation arises from the large difference in the densities of the gas and liquid. In order to represent a free surface or an interface in a two-phase fluid, a function, f , is defined.

The value of f is unity at any point occupied by one particular phase, say the primary phase, and zero otherwise. The average value of f in a cell would then represent the volume fraction of the cell that is occupied by the primary phase. Thus, the VOF method provides the coarse interface information and requires only one storage word for each computational cell, which is consistent with the storage requirements for all other dependent variables.

A single momentum equation is solved throughout the domain, and the resulting velocity field is shared among the phases.^[15] The momentum equation is dependent on the volume fraction through the phases' volume-fraction-averaged fluid properties, namely, density and viscosity, ρ and μ , respectively, which implies an interface. These averaged fluid properties are used to monitor the dynamics of the interface. However, when a large discontinuity in properties is involved, numerical difficulties may arise in identifying an *exact* interface and defining the fluid properties. Thus, instead of solving the density continuity equation directly, the volume fraction of fluid, f , is used to identify the interface.

Since turbulence plays a major role in the flotation treatment process, the momentum equations are modified to describe the effects of turbulent fluctuations of velocity and scalar quantities using Reynolds' time averaging procedure supplemented by the standard k - ϵ turbulence model. Modeling turbulent flows requires appropriate modeling procedures to describe the effects of turbulent fluctuations of velocity and scalar quantities on the basic conservation equations. Many models with varying complexity have been proposed ranging from the simple mixing length model^[16] to the more sophisticated large eddy simulations.^[16,17] The widely used k - ϵ model^[18] provides a compromise between the two extremes. The k - ϵ turbulence model is an eddy viscosity model in which the Reynolds stresses are assumed proportional to the mean velocity gradients, with the constant of proportionality being the turbulent viscosity, μ_t .

III. SOLUTION PROCEDURE AND BOUNDARY CONDITIONS

The fluid-flow pattern, the gas-bubble distribution, and the turbulence dissipation rate in a melt-treatment reactor are determined using the model presented in the previous section. The VOF free surface model in a commercial fluid-dynamics code* is employed in the simulation. A nonuni-

*FLUENT V4.4 is marketed by Fluent Inc. (Lebanon, NH).

form grid is used throughout the domain; however, the grid-node density is made higher close to the free surface and around the gas inlet region. In an Eulerian mesh, the flux of f moving with the fluid through a cell must be computed. However, standard finite-difference approximations would lead to smearing of the f function and interfaces would lose their definition. Fortunately, f being a function with values between zero and one permits the use of a flux approximation that preserves its discontinuous nature. This approximation is known as a donor-acceptor approximation.^[15]

The semi-empirical "wall-function" is used to approximate the shear stress due to the "no-slip" condition at all solid surfaces, and the values of k and ϵ at the walls are taken as those derived from the assumption of an equilibrium

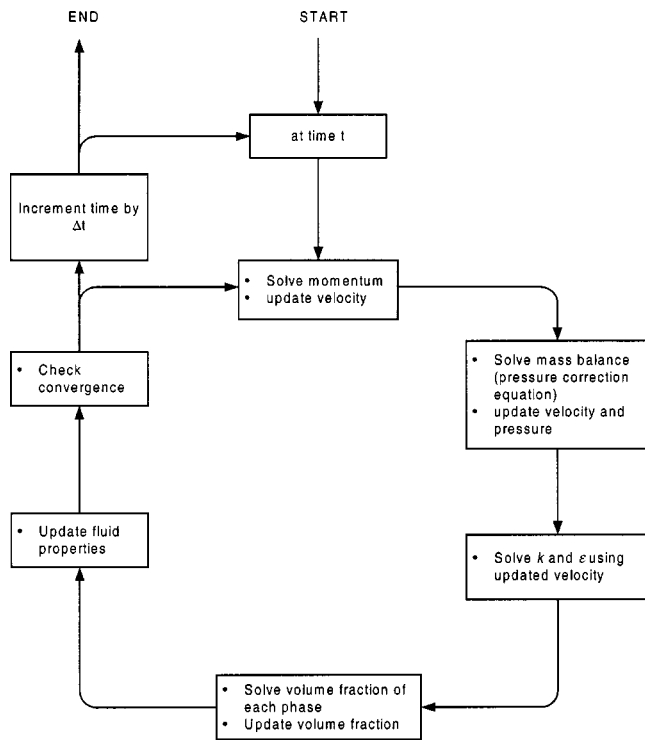


Fig. 2—Overview of the solution procedure.

boundary layer. At the gas inlet into the melt, the radial and tangential components of velocity are assumed uniform. At the gas exit from the reactor's top, diffusion fluxes of all flow variables in the direction normal to the exit plane are assumed zero. The impeller is simulated by a wall that rotates with a velocity that is defined by specifying the velocity component in the circumferential direction. Whenever symmetry exists, symmetry boundary conditions may be used, *i.e.*, assuming zero flux for all variables across the symmetry boundary. Figure 2 shows a block diagram of the solution procedure.

IV. APPLICATION OF THE MATHEMATICAL MODEL

The mathematical formulation outlined in the preceding sections was used to study the fluid-flow behavior inside a holding furnace during flotation treatment. The analysis was performed on a cylindrical furnace 0.6 m in diameter and 1-m high. The initial melt depth in the furnace was 0.75 m. Gas was purged into the melt through twelve 20-mm diameter side holes distributed evenly around the cylindrical impeller and located midway up its height. The diameter of the rotor shaft was 60 mm, the diameter of the cylindrical impeller was 200 mm, and its height was 270 mm. The clearance between the impeller bottom and the furnace bottom is 105 mm. A two-dimensional axisymmetric geometry was used to simulate the process, and the holes in the impeller were modeled by 20-mm slits. The purged gas was introduced into the computational domain outside the holes. In order to reduce the computational complexity and to simulate the free surface of the melt, a layer of argon gas was assumed on top of the melt. A 115×30 nonuniform grid was used

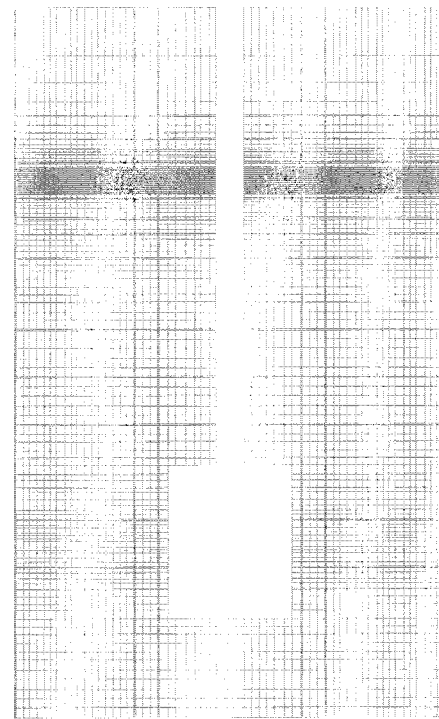


Fig. 3—Computational domain showing nonuniform grid.

Table I. Design of the Experiment

Factor	Level 1	Level 2
Rotation speed, rpm	675	350
Gas flow rate, L/min	36	15
Cycle (rotation direction), s	0	25
Purge duration, min	10	20

in the simulation, as shown in Figure 3. The process parameters that most significantly affect the efficiency of a rotary degasser are the purging gas flow rate, the rotation speed of the impeller, the duration of gas purging, and the reversal of the direction of impeller rotation. A statistically robust computer experiment that includes these process parameters as variables was designed and used to optimize a batch rotary degassing process. The molten metal was an aluminum alloy held at 750 °C in an electric furnace, and the purging gas was high purity argon. In order to extract the maximum amount of unbiased information from as few simulations as possible, a full factorial statistical design technique, the Taguchi method, was used.^[19,20] The experiment matrix was based on an L_8 orthogonal array with two levels at each factor, as shown in Table I. Table II shows the Taguchi L_8 layout along with the calculated mean turbulence dissipation rate. The mean values of the turbulence dissipation rate are computed as a volume-weighted average of the turbulence dissipation rate. The volume-weighted average considers the cell size differences and, thus, yields an average value that accounts for the spatial distribution of the variable.

Figure 4 shows the calculated velocity vectors for the reactor with the impeller rotating at 675 rpm and a gas flow rate of 36 L/min at two different purging times. These plots show the characteristic circulation patterns that are expected in mechanically stirred melt treatment systems. The velocity

Table II. Taguchi L_8 Layout and Simulation Results

Factor	ppm, A	Flow Rate L/Min, B	A × B	Cycle s, C	A × C	B × C	D	Mean Dissipation rate, m^2/s^3
Trial/column	1	2	3	4	5	6	7	(y)
1	675	36	1	0	1	1	10	23.09
2	675	36	1	25	2	2	20	31.51
3	675	15	2	0	1	2	20	7.67
4	675	15	2	25	2	1	10	26.43
5	350	36	2	0	2	1	20	0.1542
6	350	36	2	25	1	2	10	0.1729
7	350	15	1	0	2	2	10	0.1448
8	350	15	1	25	1	1	20	0.1644

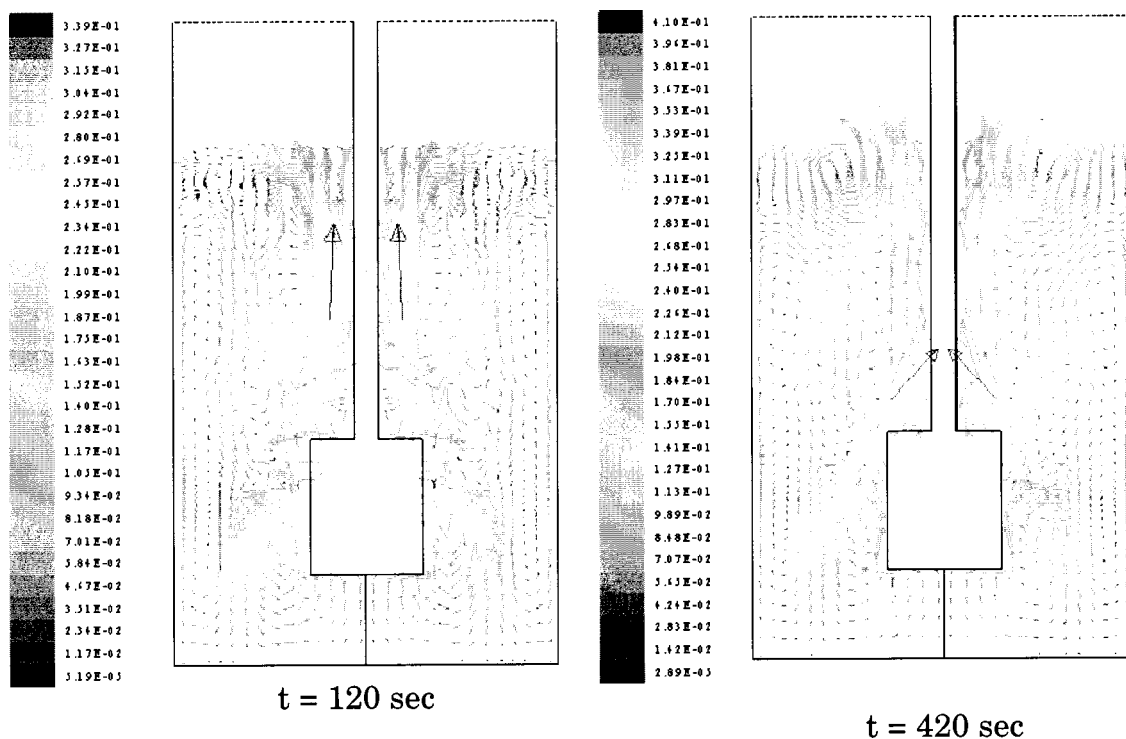


Fig. 4—Aluminum flow field in a conventional flotation reactor with impeller rotating at 675 rpm and gas flow rate of 36 L/min.

vectors near the rotor shaft are the highest in magnitude because of the upward motion of the gas bubbles. Near the free surface, the radial component of the velocity becomes significant at the lower purge time. However, at the higher purge time, a recirculation zone forms just below the free surface.

Figure 5 shows the argon gas distribution in the melt treatment furnace at two different gas purge times. The average volume fraction of argon gas in the reactor is calculated to be 0.0431.

Velocity vectors and gas distributions for a reverse-rotation** flotation reactor are shown in Figures 6 and 7, respec-

**Reverse rotation in rotary degassing was first introduced by Apogee, Inc. (Pittsburgh, PA).^[21] The impeller rotates clockwise for a predetermined period, then counterclockwise for an equal period. Here, the period was taken to be 25 s including a 1 s transition time.

tively. In the reverse-rotation flotation reactor, the velocity vector near the free surface is radial. In addition, the circulation zone inside the furnace is more prominent, thereby,

ensuring good mixing of the melt and enhancing the probability of interaction between inclusions and gas bubbles. The average volume fraction of argon gas in this reactor is 0.046.

Figures 8 and 9 show the computed turbulence dissipation rate for the conventional and the reverse-rotation flotation reactors, respectively. These plots show that the turbulence dissipation rate is nonuniform in both flotation reactors, being highest near the impeller and its shaft. However, in the reverse-rotation reactor, the higher dissipation rates are more spread and cover a larger volume of the furnace than in the traditional reactor. It should be noted that the absolute values of the dissipation rate in the rotary degasser are in the range of 0.01 to $2 \times 10^4 m^2/s^3$. These values are quite high in comparison to those obtained using only a gas bubble stirring system, e.g., a porous plug or a stationary lance.^[22] The mean values of turbulence dissipation rates are 23.09 m^2/s^3 in the conventional flotation reactor and 31.51 m^2/s^3 in the reverse-rotation reactor operating at the conditions given in Table II.

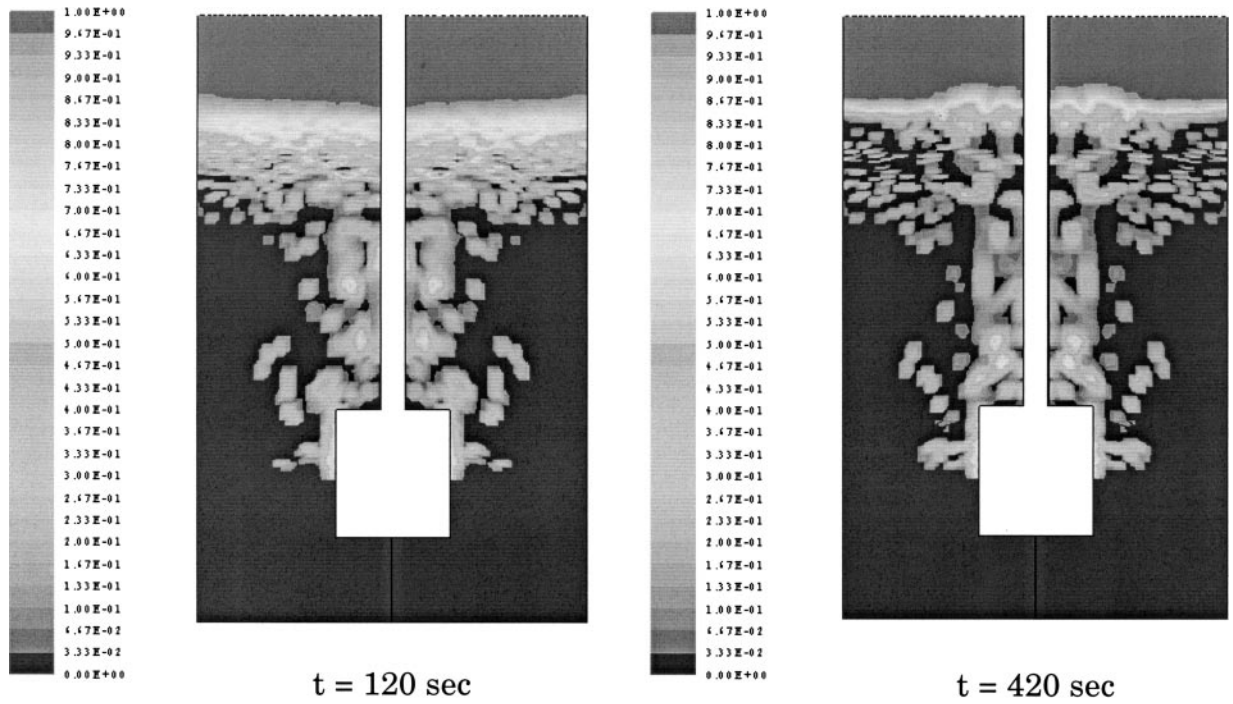


Fig. 5—Argon gas distribution in the melt treatment furnace in a conventional degasser rotating at 675 rpm.

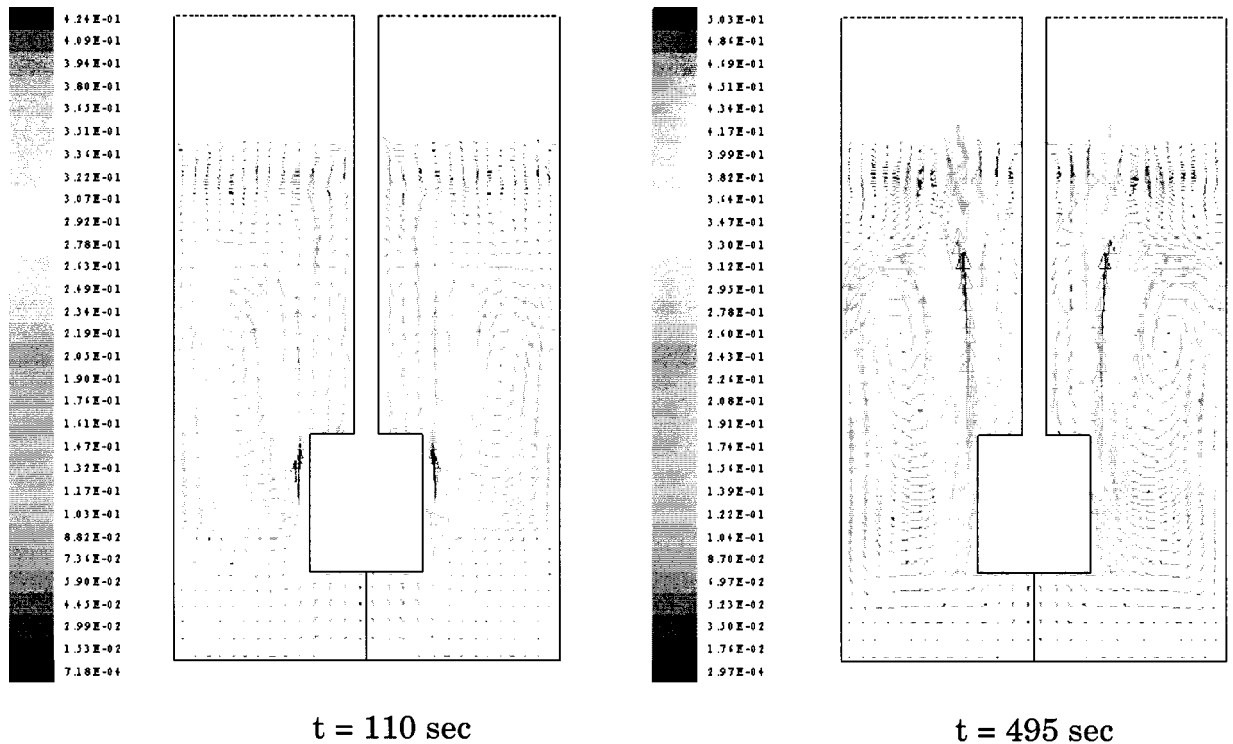


Fig. 6—Aluminum melt flow field in a reverse rotation flotation reactor with impeller rotating at 675 rpm (cycles every 25 s) and gas flow rate of 36 L/min.

Analysis of variance (ANOVA) was performed on the data in order to identify the effect of each process parameter and each interaction on the variance in the mean turbulence-energy dissipation rate. The procedure for performing ANOVA is detailed elsewhere.^[19,20] Results of the pooled analysis of variance are shown in Table III. The percent contribution is an indication of the relative influence of a

particular parameter or an interaction to affect variation in the mean turbulence-energy dissipation rate. Table III shows that for the system modeled, at the levels studied, the process parameter that affects variation in the mean turbulence-energy dissipation rate most significantly is the rotation speed. Its relative contribution to the variation is about 74 pct. Periodic reversal of the rotation direction also has an effect

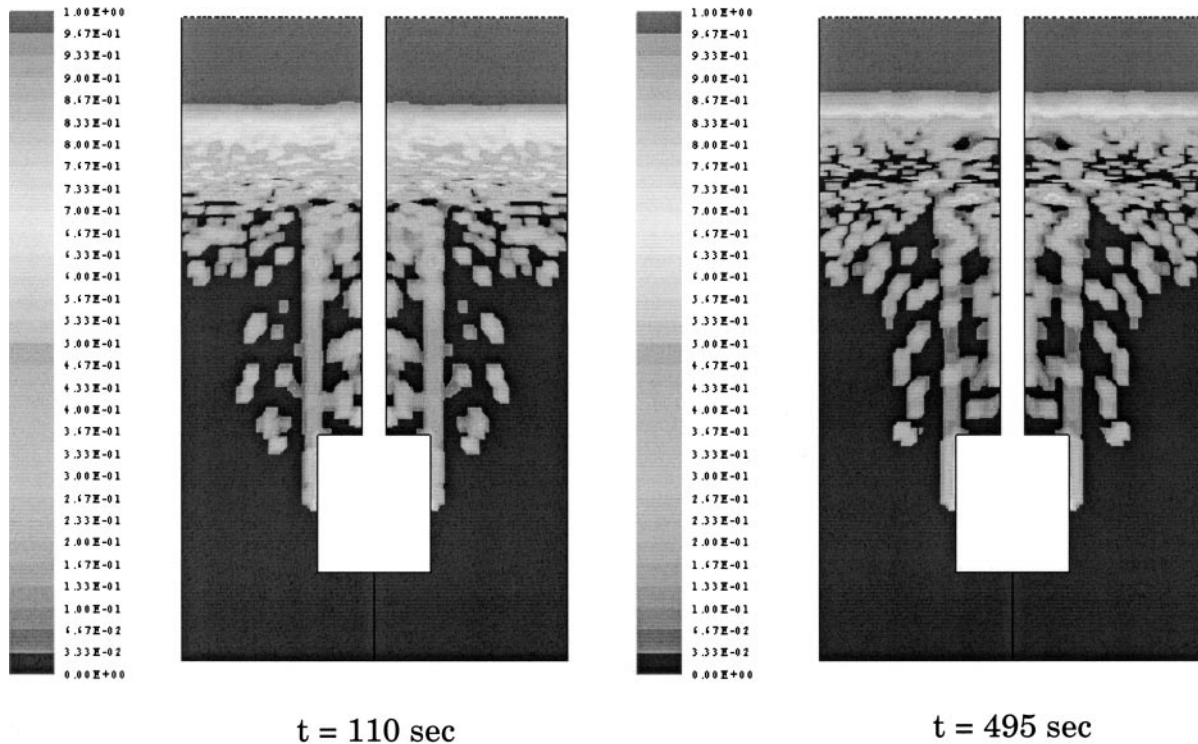


Fig. 7—Argon gas distribution in the melt treatment furnace in a reverse rotation flotation reactor with impeller rotating at 675 rpm (cycles every 25 s) and gas flow rate of 36 L/min.

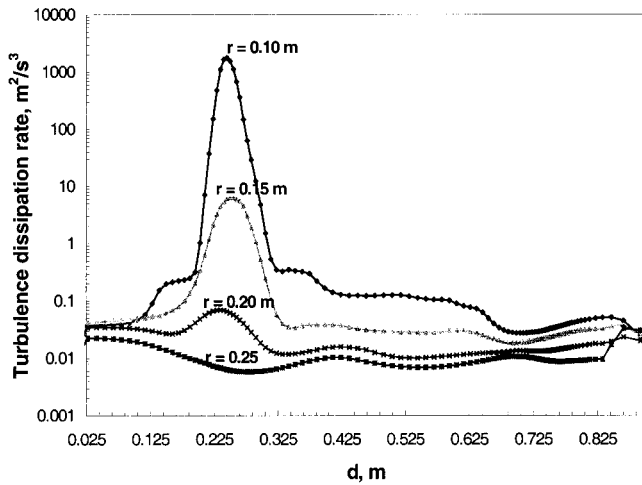


Fig. 8—Turbulence dissipation rate as a function of the distance from the furnace bottom (d) and radial distance from the center of the furnace (r) for a conventional flotation reactor at $t = 420$ s, 675 rpm rotation speed, and 36 L/min gas flow rate.

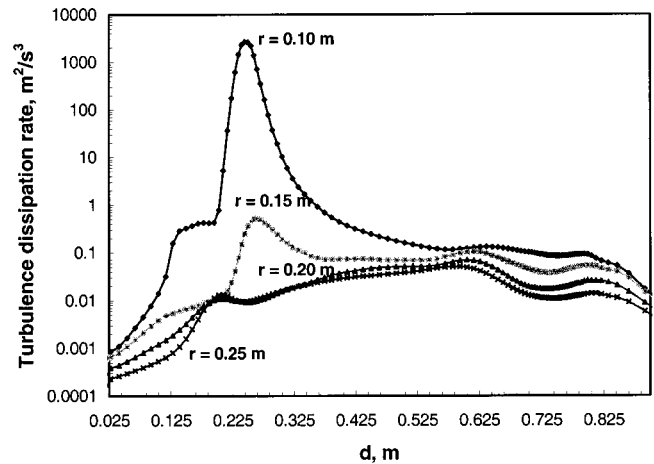


Fig. 9—Turbulence dissipation rate as a function of the distance from the furnace bottom (d) and radial distance from the center of the furnace (r) of a reverse rotation flotation reactor at $t = 420$ s, rotation 675 rpm, and gas flow rate 36 L/min.

on the mean turbulence-energy dissipation rate contributing over 6 pct to the variance. Higher rotation speeds and periodic reversal of the rotation direction increase the mean turbulence-energy dissipation rate. All other process parameters seem to have comparatively insignificant effects on the mean turbulence-energy dissipation rate. The percent contribution due to the error term provides an estimate of the adequacy of the experiment.^[19,20] If the error term is low, *i.e.*, 15 pct or less, it is assumed that no important factors were omitted from the design of the experiment and computational errors were insignificant. On the other hand,

if the percent contribution due to the error term is high, then some important factors were omitted, or computational errors were excessive. The percent contribution due to the error term in this analysis is about 7 pct, which is acceptable.

V. SUMMARY

A mathematical model for simulating the multiphase flow field inside a rotating impeller flotation unit for removal of solid inclusion from molten metal has been developed. The model estimates the turbulence-energy dissipation rate and

Table III. Pooled ANOVA Table for Turbulence Dissipation Rate

Factor	Sum of Squares	Variance	Percent Contribution
Rotation speed	969.587	969.586	74.37
Gas flow rate	52.580	52.579	3.05
Speed × gas flow rate	52.397	52.396	3.04
Rotation direction	92.547	92.547	6.16
Speed × rotation direction	92.027	92.026	6.12
Gas flow rate × rotation direction	(13.345)	pooled	—
Duration	(13.340)	pooled	—
Error	26.685	13.342	7.26
Total	1285.823	—	100.00

the purge gas volume fraction in the treatment furnace. In addition to providing insight into the physical mechanisms underlying the rotating impeller flotation process, the mathematical model was used to simulate a batch-type rotary degasser. Since a high mean turbulence-energy dissipation rate implies more interparticle collisions and a higher probability of particle attachment to gas bubbles, and, consequently, more efficient performance of the rotary degasser,^[12] the simulations were used to determine the optimum parameters for operating a small batch-type rotary degasser. The simulation results indicate that the impeller's rotating speed has the most significant effect on the turbulence-energy dissipation rate; consequently, it is the most important process parameter. The simulations also indicate that periodic reversal of the impeller's rotation direction has a positive effect on the process efficiency. The model developed here is used in part II^[12] to simulate inclusion removal from molten aluminum in a standard as well as a reverse-rotation rotary degasser.

REFERENCES

1. T.A. Engh: *Principles of Metal Refining*, Oxford University Press, New York, NY, 1992, pp. 1-35.
2. G. Sachs, A.W. Dana, and L.J. Ebert: *AFS Trans.*, 1947, vol. 55, p. 102.
3. Q.G. Wang, D. Apelian, and J.R. Griffiths: *1st Int. Aluminum Symp.*, Rosemont, IL, 1998.
4. G.R. Wakefield and R.M. Sharp: *Mater. Sci. Technol.*, 1996, vol. 12, pp. 518-22.
5. C. Nyahumwa, N.R. Green, and J. Campbell: *AFS Casting Congr.*, Atlanta, GA, 1998.
6. R. Cook, M.A. Kearns, and P.S. Cooper: *Light Met.*, 1997, pp. 809-14.
7. S.T. Johansen and F. Boysan: *Metall. Trans. B*, 1988, vol. 19B, pp. 755-64.
8. O.J. Ilegbusi and J. Szekely: *Iron Steel Inst. Jpn. Int.*, 1990, vol. 30, pp. 731-39.
9. O.J. Ilegbusi and J. Szekely: *Int. Symp. on Injection in Process Metallurgy*, 1991, TMS, Warrendale, PA, pp. 1-34.
10. S.T. Johansen, A. Fredriksen, and B. Rasch: *Light Met.*, 1995, pp. 1203-06.
11. B.I. Hop, S.T. Johansen, and B. Rasch: *EPD Congr.*, 1996, TMS, Warrendale, PA, pp. 647-56.
12. M. Maniruzzaman and M. Makhlof: Worcester Polytechnic Institute, Worcester, MA, unpublished research, 2000.
13. C. Crowe, M. Sommerfeld, and Y. Tsuji: *Multiphase Flows with Droplets and Particles*, CRC Press, Boca Raton, FL, 1997.
14. FLUENT: *FLUENT User's Guide*, FLUENT Inc., Lebanon, NH, 1996, vols. 2-4.
15. C.W. Hirt and B.D. Nichols: *J. Comput. Phys.*, 1981, vol. 39, pp. 201-25.
16. O.J. Ilegbusi, M. Iguchi, and W. Wahnsiedler: *Mathematical and Physical Modeling of Materials Processing Operations*, Chapman & Hall/CRC, Boca Raton, FL, 1999.
17. J. Derksen and H.E.A.V. d. Akker: *AIChE J.*, 1999, vol. 45, pp. 209-21.
18. B.E. Launder and D.B. Spalding: *Lectures in Mathematical Models of Turbulence*, Academic Press, London, 1972.
19. P.J. Ross: *Taguchi Techniques for Quality Engineering*, McGraw-Hill Book Company, New York, NY, 1988.
20. R.K. Roy: *A Primer on the Taguchi Method*, Society of Manufacturing Engineers, Dearborn, MI, 1990.
21. C.E. Eckert: U.S. Patent No. 5,616,167, 1997.
22. O.J. Ilegbusi and J. Szekely: *Metall. Trans. B*, 1990, vol. 21B, pp. 183-90.